MEMS-Nav: A MEMS-Grade Dataset for Navigation Research

Journal Title
XX(X):1–7

DOI: 10.1177/ToBeAssigned
www.sagepub.com/
SAGE

James Brodovsky[1], Philip Dames [1]

Abstract

This paper describes a dataset and toolbox for research and education in the field of navigation using MEMS-grade sensors. Many other such datasets either are collected in a fairly small scale laboratory or field setting (typical of the robotics and unmanned systems community), or they focus on high-end sensors (typical of the marine and aerospace communities). In contrast, this dataset splits the difference: it is collected on what might be the most ubiquitous type of sensor configuration — the MEMS-grade IMU and GPS antenna on most modern cell phones — and contains longer term trajectories comparable to the marine and aerospace communities. It's primary contribution it to provide a dataset that is both accessible and representative of real-world navigation problems for education as well as simulation of conditions of GPS/GNSS degradation, spoofing, and intermittent availability to enable research into alternative navigation techniques.

Keywords

inertial navigation, MEMS-grade sensors, dataset, IMU, GPS, GNSS

Introduction

Inertial navigation systems (INSs) are widely used in various applications, including the robotics, aerospace, maritime, and automotive industries. These systems rely on a combination of inertial measurement units (IMUs) and external state feedback. The general architecture of a modern INS is to use the angular rate and specific force measurements from the IMU to propagate the state estimate over time. IMUs (even high quality ones) are nonetheless noisy sensors and integrating noise values twice eventually leads to substantial accumulation of error in the position and orientation estimates. This error is corrected by some sort of external state feedback often provided by the global navigation satellite system (GNSS), external beacons or markers, or by mapping landmarks via computer vision, lidar, or other sensing modalities.

However the scale of the navigation problem in each application has facilitated different approaches to data collection and processing. While Bayesian navigation techniques have their origin in aerospace and maritime applications, the robotics and unmanned systems community has recently been making strides in the development of various autonomous navigation and localization applications using the same basic filters. This in turn has influenced the types of data collected by researchers in these fields.

An additional factor is the long term reliance and overall quality of traditional GNSS-INS systems. Even relatively inexpensive commercial grade systems can achieve high levels of accuracy in optimal conditions. Accuracy on the order of a few meters (or even centimeters) is common and is often sufficient for a vehicle that has footprint of tens or hundreds of meters such as a commercial airliner or container ship. However, these systems' reliance on the GNSS makes them subject to various forms of GNSS signal degradation, including spoofing, intermittent availability, and other environmental factors that can affect the accuracy of the state feedback measurements. This has led to an increased interest in alternative methods of providing positioning, navigation, and timing (PNT) estimates that do not rely solely on GNSS and are thus subject to a single point of failure.

Problem

Overview of available datasets

Researchers and practitioners require access to quality datasets that capture or simulate the complexities of real-world navigation scenarios. Many such datasets exist that capture some aspects of these challenges, however they frequently rely on higher-end sensors, are proprietary even if still open-access (Waymo LLC 2025), or are collected in a fairly small scale laboratory or field setting. Additionally, the prominence of robotics and autonomy research groups publishing datasets in this field has led to a focus on datasets that are collected with the intent on developing a new capability (visual inertial odometry, simultaneous localization and mapping, et cetera) by leveraging and incorporating additional information about the local environment via additional sensors. This has also influenced the scale of datasets collected and it is common to see datasets that are collected on a small scale (such as in a building or laboratory) or in a small area (such as a campus

[1]Temple University

Corresponding author:
James Brodovsky, Temple University, Philadelphia, PA 19122, USA
Email: jbrodovsky@temple.edu

or urban setting). A brief survey of these datasets is shown in Table 1.

In contrast, many traditional navigation problems do not have such information available to them in their environment. The aerospace and marine communities frequently operate in open environments with little availability of notable landmarks. Outside the explicit limited context of basic visual flight rules the reliance on inertial navigation and radio based position feedback is increasingly pronounced. Aviation in particular has a long history of using radio navigation aids such as very high frequency omnidirectional range station (VOR) (Anderson 1965), non-directional beacon (NDB) (Kayton and Fried 1997, Chapter 4.4.2), and distance measuring equipment (DME) (Kayton and Fried 1997, Chapter 4.4.6) navigation aids to provide position feedback to pilots through manual calculations. In modern practice, these systems are being phased out in favor of attitude heading and reference systems (AHRS) and INSs that rely on the GNSS to provide position and orientation information (Groves 2008, Chapter 6). However, these systems can be subject to various forms of degradation, including spoofing, intermittent availability, and other environmental factors that can affect the accuracy of the position estimates (Miralles et al. 2020; Santamaria).

On the opposite end of the use-case spectrum, the maritime community also faces similar issues with the reliance on GNSS or radio navigation aides. Surface vessels face similar challenges to aircraft but sub-surface vessels face the additional challenge of not being able to use the GNSS at all (Zhang et al.). Sub-surface vessels, ranging from military submarines to scientific unmanned underwater vessels, rely on an onboard INSs and other sensors to provide position and orientation information. Like all INS systems, these systems require external feedback in order to bound error. In contrast to surface vessels and aircraft, common means of obtaining such a position fix are typically at odds with the operational constraints of these platforms. The canonical example is that of a military submarine that must remain undetected and therefore cannot surface to obtain a GNSS fix.

Challenges in collecting representative data

Despite the breadth of datasets available, collecting representative data in GNSS-denied or degraded environments remains an open challenge. True denial scenarios—such as underwater or intentionally jammed conditions—are often logistically difficult, costly, or unsafe to replicate at scale. Even partial degradations, such as intermittent satellite visibility in urban canyons or under dense foliage, are highly environment-dependent and can be inconsistent from one experiment to another. This makes it difficult for researchers to obtain reproducible datasets that isolate the effects of GNSS degradation on navigation performance, particularly when using low-cost MEMS-grade sensors. As a result, the majority of available datasets continue to reflect ideal or near-ideal GNSS availability, limiting their utility for evaluating robustness in contested or constrained environments.

To address this gap, a complementary approach is to begin with high-quality, reproducible datasets and then systematically degrade the GNSS measurements in a controlled manner. This allows researchers to emulate spoofing, jamming, or intermittent availability while maintaining a consistent ground-truth reference. The ability to inject controlled degradations makes it possible to compare algorithms fairly, evaluate sensitivity to different types of GNSS disruptions, and benchmark alternative navigation strategies such as geophysical aiding or vision-based localization. Importantly, this reproducibility provides an avenue for broader adoption in both research and education: students and practitioners can explore realistic denial conditions without requiring access to specialized facilities or equipment, while developers can rigorously test robustness under a spectrum of degraded navigation scenarios

The MEMS-Nav Dataset and Strapdown Simulator

This paper presents the MEMS-Nav dataset. The dataset was collected using a variety of smartphones all of which had an internal IMU board that contained accelerometers, gyroscopes, magnetometers, and a barometer, paired with a GPS antenna using the Sensor Logger application (Choi 2020). There were a variety of vehicles used to collect the data but the majority of the data was collected using a car and typically on highway driving conditions. The raw recording measurements were synchronized and contain the following measurements from GNSS processing:

- **Latitude** — WGS 84 degrees latitude
- **Longitude** — WGS 84 degrees longitude
- **Altitude** — WGS 84 altitude in meters
- **Speed** — Ground speed in meters per second
- **Horizontal Accuracy** — Horizontal accuracy in meters
- **Vertical Accuracy** — Vertical accuracy in meters

from IMU processing:

- **Bearing** — Magnetic bearing (compass) in degrees
- **Bearing Accuracy** — Bearing accuracy in degrees
- **Angular Rates** — Angular rates in radians per second (`gyro_x`, `gyro_y`, `gyro_z`)
- **Magnetic Field Vector** — Magnetic field in microteslas (`mag_x`, `mag_y`, `mag_z`)
- **Gravity Vector** — Gravity vector in meters per second squared (`grav_x`, `grav_y`, `grav_z`)
- **Pressure** — Barometric pressure in millibars

and derived quantities:

- **Relative Altitude** — meters, relative change in altitude derived from barometric pressure
- **Attitude (Euler Angles)** — roll, pitch, and yaw in degrees
- **Attitude (Quaternion)** — quaternion representation of the attitude (`qx`, `qy`, `qz`, `qw`)
- **Linear Acceleration** — Linear acceleration in meters per second squared (`acc_x`, `acc_y`, `acc_z`)

This dataset was processed using `strapdown-rs` (Brodovsky 2025) to develop the truth dataset and simulated degraded trajectories. The dataset, toolbox, and simulator are

Table 1. Short summary of some publicly available navigation datasets. Most datasets focus on providing feedback via the structure of the surrounding environment and are typically recorded on a laboratory, campus, or urban setting.

Dataset	Platform	Ground Truth	Scale
MIT DARPA Huang et al. (2010)	Car	GPS+INS	Urban
Ford Campus Pandey et al. (2011)	Car	GPS+INS	Campus
KITTI Geiger et al. (2013)	Car and Robot	GPS+INS	Urban
Oxford RobotCar Maddern et al. (2017)	Car	GPS+INS	Urban
KAIST Urban Jeong et al. (2019)	Car	SLAM	Urban
GFINS Yampolsky et al. (2024)	Car	GPS+INS	Campus
New College Smith et al. (2009)	Handheld	SLAM	Campus
Newer College Ramezani et al. (2020)	Handheld	SLAM	Campus
UMA-VI Zuñiga-Noël et al. (2020)	Handheld	SLAM	Campus
UZH FPV Delmerico et al. (2019)	UAV	GPS+INS	Campus
TUM VI Schubert et al. (2018)	Handheld	SLAM	Campus
Penn Fast Flight Sun et al. (2018)	UAV	GPS	Laboratory
EuRoC Burri et al. (2016)	UAV	Laser Tracker	Campus
NTU VIRAL Nguyen et al. (2022)	UAV	Laser Tracker	Campus
ANSFL Shurin et al. (2022)	Mixed	GPS+INS	Regional

designed to be both accessible and representative of real-world conditions. The dataset is collected using MEMS-grade sensors, which are commonly found in modern smartphones and other consumer electronics. This makes the dataset more relatable and applicable to a wider audience, including researchers and developers working with low-cost navigation systems.

The dataset has three primary contributions. First, the preprocessed input recordings that can be used for the development of alternative positioning, navigation, and timing (AltPNT) technology. Second, a 'truth' dataset that is generated using a strapdown mechanization approach with GNSS position and velocity measurements as well as barometric altitude fused via an Unscented Kalman Filter INS. This truth dataset is intended to provide a reference 'ground truth' for evaluating the performance of other navigation algorithms. The input dataset and corresponding truth dataset can be used as a benchmark for developing and testing new algorithms as well as an educational resource for autonomous navigation courses. Third, the dataset contains a variety of simulated environmental conditions related to the GNSS signal (e.g. an intermittent signal due to jamming, a degraded signal due to interference, et cetera) that serve as examples of what the simulator is capable of generating. This is intended to provide a useful resource for researchers investigating GNSS-denied navigation techniques.

Reference INS Implementation

When dealing with noisy sensors and probabilistic navigation and state estimation techniques a word must be said about what is considered 'truth' and what you compare your estimates against to measure error. Fundamentally, these techniques all rely on quantities that are considered noisy and probabilistic as such it is important to establish both an estimate and a certainty.

Frequently, a highly accurate external reference, such as motion capture systems or GNSS measurements is used and this is perfectly acceptable when the goal is to evaluate a navigation or simultaneous localization and mapping (SLAM) system that does not use these measurements. Additionally, Bayesian filtering techniques often produce more accurate and more confident estimates from combining multiple noisy measurements. Both the raw measurements (the 'input' dataset) and the filtered dataset ('truth') are provided as a reference. User are free to use either the GNSS measurements or the estimated state as their source of truth for error comparison.

Coordinate and state definitions The local level frame is defined as a frame that is tangent to the Earth's surface with axes pointed towards the Earth's north pole, eastward direction, and a vertical axis pointing normal to the surface. These axes are typically configured as a right handed

orthonormal frame of North-East-Down or East-North-Up. The typical nine-state NED/ENU navigation state vector is used in this implementation. The state vector is defined as:

$$x = [p_n, p_e, p_d, v_n, v_e, v_d, \phi, \theta, \psi]$$

where:

- p_n, p_e, and p_d are the WGS84 geodetic positions (degrees latitude, degrees longitude, meters relative to the ellipsoid)
- v_n, v_e, and v_d are the local level frame (NED/ENU) velocities (m/s) along the north axis, east axis, and vertical axis
- ϕ, θ, and ψ are the Euler angles (in radians) representing the orientation of the body frame relative to the local level frame (XYZ Euler rotation)

INS mechanization IMUs sense motion relative to the inertial reference frame of the Earth. This is a coordinate frame that is non-rotating and centered at the Earth's center of mass. It is useful for mathematical derivations but is not practical for navigation. As such the IMU output must be transformed into a more useful frame. Historically, this was done using a gimbaled platform that mechanically stabilized a mechanical IMU consisting of spinning-mass gyroscopes and pendulous accelerometers and kept it aligned with the desired navigation frame. Such a setup is referred to as an INS "mechanization." Fiber-optic gyroscopes (FOG), ring laser gyroscopes (RLG), and microelectromechanical system (MEMS) IMUs have yielded comparatively cheaper and more accurate sensors (Eberlein and Savage 1975) that can be used to sense the same angular rates and specific forces as a mechanical IMU but without the need for a mechanically stabilized platform. This allows for the IMU to be rigidly mounted or "strapped down" to the vehicle body and use a digital computer to perform the necessary coordinate transformations. This approach is referred to as a "strapdown mechanization" (Garg et al. 1978) and is the architecture adopted for the reference INS implementation.

Navigation equations in the Local-Level Frame The reference INS implements the navigation equations in the Local-Level Frame according to Groves (2008) assuming a strapdown mechanization. These equations form the basis of the forward propagation step (motion/system/state-transition model) of the INS's filter and are executed in three steps: the attitude update, the velocity update, and the position update.

First, we represent the attitude of the body frame (b) with respect to the local level frame (n) as a rotation matrix $\mathbf{C}_b^n$. This representation allows for easier computation through matrix calculations. Similarly, the transport rate $\mathbf{\Omega}_{en}^n$ representing the rotation of the local level frame with respect to the Earth-fixed frame (e), the Earth's rotation rate $\mathbf{\Omega}_{ie}^e$, and the angular rate $\mathbf{\Omega}_{ib}^b$ representing the rotation of the body frame with respect to the inertial frame (i) are modeled as skew-symmetric matrices:

$$\boldsymbol{\omega} = \begin{bmatrix} a \\ b \\ c \end{bmatrix} \rightarrow \mathbf{\Omega} = \begin{bmatrix} 0 & -c & b \\ c & 0 & -a \\ -b & a & 0 \end{bmatrix}$$

The attitude update equation is given by:

$$\mathbf{C}_b^n(+) \approx \mathbf{C}_b^n(-)\left(\mathbf{I} + \mathbf{\Omega}_{ib}^b t\right) - \left(\mathbf{\Omega}_{ie}^e - \mathbf{\Omega}_{en}^n\right)\mathbf{C}_b^n(-)t$$

where t is the time differential and $\mathbf{C}(-)$ is the prior attitude. These attitude matrices are then used to transform the specific forces from the IMU:

$$\mathbf{f}_{ib}^n \approx \frac{1}{2}\left(\mathbf{C}_b^n(+) + \mathbf{C}_b^n(-)\right) f_{ib}^b$$

Next, the velocity is updated by:

$$\mathbf{v}(+) \approx \mathbf{v}(-) + \left(\mathbf{f}_{ib}^n + \mathbf{g}_b^n - \left(\mathbf{\Omega}_{en}^n - \mathbf{\Omega}_{ie}^e\right)\mathbf{v}(-)\right)t$$

Finally, the base position states are updated in three steps. First update the altitude:

$$p_d(+) = p_d(-) + \frac{1}{2}\left(v_d(-) + v_d(+)\right)t$$

Next, update the latitude:

$$p_n(+) = p_n(-) + \frac{1}{2}\left(\frac{v_n(-)}{R_n + p_d(-)} + \frac{v_n(+)}{R_n + p_d(+)}\right)t$$

Finally, update the longitude:

$$p_e(+) = p_e(-) + \frac{1}{2}\left(\frac{v_e(-)}{(R_e + p_d(-))\cos p_n(-)} \ldots + \frac{v_e(+)}{(R_e + p_d(+))\cos p_n(+)}\right)t$$

where and R_n and R_e are the radii of curvature in the north (meridional) and east (prime vertical) directions respectively.

The filter then updates the mean and covariance using a loosely coupled architecture. In such an architecture, the GNSS receiver produces a position and velocity estimate that is directly compared to the filter's state estimate. Additionally, the onboard barometer's estimate of relative altitude is included to provide additional feedback into the vertical channel.

GNSS Degradation Models

To enable systematic evaluation under contested navigation conditions, the toolbox provides models that act at two layers: scheduling (when GNSS fixes are delivered) and fault injection (how those fixes are corrupted). These can be used independently or in combination, allowing the same high-quality dataset to be replayed under a wide variety of degraded scenarios.

At the scheduling level, three modes are supported. The *pass-through* scheduler emits all measurements without modification and serves as a baseline for 'ideal' conditions. A *fixed-interval* scheduler outputs fixes at a prescribed interval (e.g., every 10 s), discarding intermediate updates to mimic reduced-rate operation caused by jamming, low-power duty cycling, or bandwidth constraints. The *duty-cycle* scheduler alternates between ON and OFF windows, reproducing periodic outages similar to those encountered in tunnels or urban canyons. These mechanisms provide control over temporal availability and can be tuned to match operational conditions.

At the measurement level, the toolbox implements several distinct corruption models. The *degraded* model applies autoregressive (AR(1)) noise processes to position and velocity (Wang et al. 2022), combined with inflated

covariance reports. This represents conditions such as multipath or low-SNR reception, where GNSS remains available but with reduced fidelity. The *slow bias* model represents "soft spoofing": a gradual drift in position and velocity along a chosen direction, potentially with stochastic and rotational components. Such errors remain plausible to a Bayesian filter and are therefore particularly insidious. The *hijack* model, in contrast, represents "hard spoofing": a constant offset applied abruptly during a specified time window, displacing the estimated trajectory onto a parallel but false path. Finally, a *combination* model allows these effects to be chained together, such as combining a slow drift with a subsequent spoofing window, to emulate complex multi-stage attacks.

An example

An example trajectory from the dataset is shown in Figure 1. This trajectory was collected using a car on predominantly highway driving conditions. The trajectory is approximately 90 minutes long and covers a distance of approximately 113 kilometers.

Using the "passthrough" scheduler and no fault injection, the reference INS produces the position error shown in Figure 2. The position error is calculated as the difference between the GNSS position measurements and the INS position estimate using a haversine distance. The haversine distance defines the great circle distance between two points (P_1, P_2) on a sphere via their latitude (ϕ) and longitude (λ)

$$d = \text{hav}(P_2 - P_1) = 2R_E \arcsin\left(\sqrt{\sin^2\frac{\phi_2 - \phi_1}{2} \ldots + \cos(\phi_1)\cos(\phi_2)\sin^2\frac{\lambda_2 - \lambda_1}{2}}\right)$$

While not necessarily as precise as GPS or a high-end INS, the reference trajectory is nonetheless a substantial improvement over using the IMU alone, and is at times able to achieve a horizontal estimate that is more accurate than the GNSS measurements themselves. The barometric altitude measurements also provide a substantial improvement over the GNSS altitude measurements and IMU, as the vertical channel is often very noisy. This reference INS trajectory can therefore be used as a reasonable ground truth for evaluating the performance of other navigation algorithms.

Using the same input recording, we then subject the GNSS measurements to a variety of degradation models as shown in Table 3. The resulting position errors are normalized to be with respect to distance traveled. These results are shown in Figure 3.

Conclusion

This paper presents the MEMS-Nav dataset, which is designed to be both accessible and representative of real-world conditions. The dataset is collected using MEMS-grade sensors, which are commonly found in modern smartphones and other consumer electronics. This makes the dataset more relatable and applicable to a wider audience, including researchers and developers working with low-cost navigation systems. The dataset is preprocessed and includes a 'truth' dataset generated using a strapdown mechanization approach with GNSS position and velocity measurements as well as barometric altitude fused via an Unscented Kalman Filter INS. This truth dataset is intended to provide a reference 'ground truth' for evaluating the performance of other navigation algorithms. The input dataset and corresponding truth dataset can be used as a benchmark for developing and testing new algorithms as well as an educational resource for autonomous navigation courses.

Additionally, the dataset contains a variety of simulated environmental conditions related to the GNSS signal (e.g. an intermittent signal due to jamming, a degraded signal due to interference, et cetera) that serve as examples of what the simulator is capable of generating as well as pre-packaged scenario results for testing. This is intended to provide a useful resource for researchers investigating GNSS-denied navigation techniques.

The processed files composing the dataset are available at https://github.com/jbrodovsky/mems-nav-dataset. The raw data files are available upon request to the corresponding author.

Acknowledgements

The author would like to thank the following people for their assistance in recording the raw data files: Beth Brodovsky, Jeremy Brodovsky, Monica Brodovsky, Bill Siegl, and Alkesh Kumar Srivastava.

References

Anderson SR (1965) Vhf omnirange accuracy improvements. *IEEE Transactions on Aerospace and Navigational Electronics* 12(1): 26–35.

Brodovsky J (2025) strapdown-rs: A simple strapdown INS implementation in rust. DOI:10.5281/zenodo.1234567. Zenodo Preprint.

Burri M, Nikolic J, Gohl P, Schneider T, Rehder J, Omari S, Achtelik MW and Siegwart R (2016) The euroc micro aerial vehicle datasets. *The International Journal of Robotics Research* 35(10): 1157–1163.

Choi TH (2020) Awesome sensor logger. Technical report. URL https://github.com/tszheichoi/awesome-sensor-logger.

Delmerico J, Cieslewski T, Rebecq H, Faessler M and Scaramuzza D (2019) Are we ready for autonomous drone racing? the uzh-fpv drone racing dataset. In: *2019 International Conference on Robotics and Automation (ICRA)*. IEEE, pp. 6713–6719.

Eberlein A and Savage P (1975) Strapdown cost trend study and forecast. Technical report.

Garg S, Morrow L and Mamen R (1978) Strapdown navigation technology: A literature survey. *Journal of Guidance and Control* 1(3): 161–172.

Geiger A, Lenz P, Stiller C and Urtasun R (2013) Vision meets robotics: The kitti dataset. *The international journal of robotics research* 32(11): 1231–1237.

Groves PD (2008) *Principles of GNSS, Inertial, and Multisensor Integrated Navigation Systems*. Artech House.

Huang AS, Antone M, Olson E, Fletcher L, Moore D, Teller S and Leonard J (2010) A high-rate, heterogeneous data set from

Table 2. Summary of GNSS degradation models implemented in the toolbox.

Layer	Model	Description	Representative Scenario
Scheduling	Pass-through	Emit all fixes unchanged.	Baseline / truth replay
	Fixed-interval	Emit fixes only at specified intervals; drop others.	Jamming, low-power mode
	Duty-cycle	Alternate ON/OFF windows of availability.	Tunnel, urban canyon
Fault Model	None	No corruption of measurement content.	Baseline
	Degraded	AR(1) correlated noise in position & velocity; inflated covariance.	Multipath, interference
	Slow bias	Gradual drift in N/E position & velocity; optional random walk and rotation.	Soft spoofing
	Hijack	Constant offset applied during a time window.	Hard spoofing attack
	Combo	Sequential application of multiple models.	Multi-stage spoofing/jam

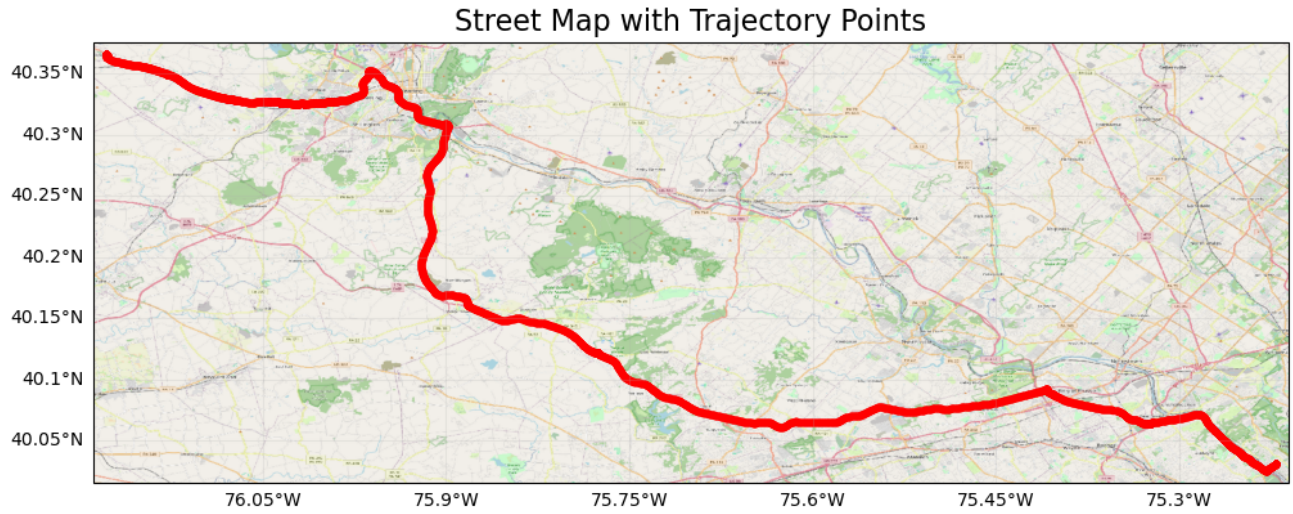

Figure 1. Example trajectory from the MEMS-Nav dataset.

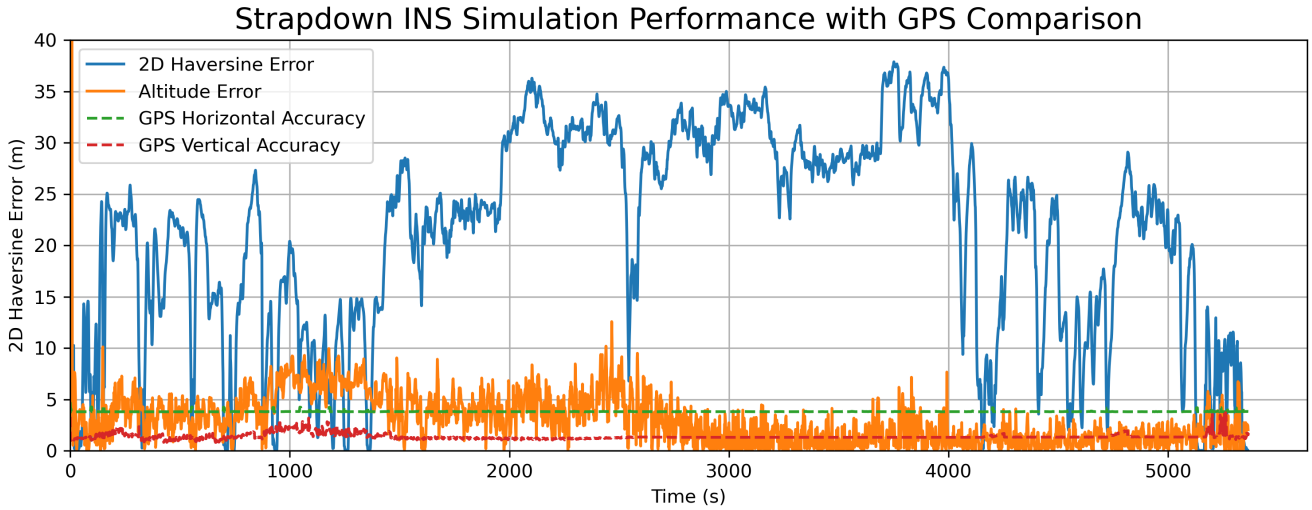

Figure 2. Position error of the reference "truth" trajectory that fuses IMU and GNSS measurements.

the DARPA urban challenge. *The International Journal of Robotics Research* 29(13): 1595–1601.

Jeong J, Cho Y, Shin YS, Roh H and Kim A (2019) Complex urban dataset with multi-level sensors from highly diverse urban environments. *The International Journal of Robotics Research* 38(6): 642–657.

Kayton M and Fried WR (1997) *Avionics navigation systems*. John Wiley & Sons.

Maddern W, Pascoe G, Linegar C and Newman P (2017) 1 year, 1000 km: The oxford robotcar dataset. *The International*

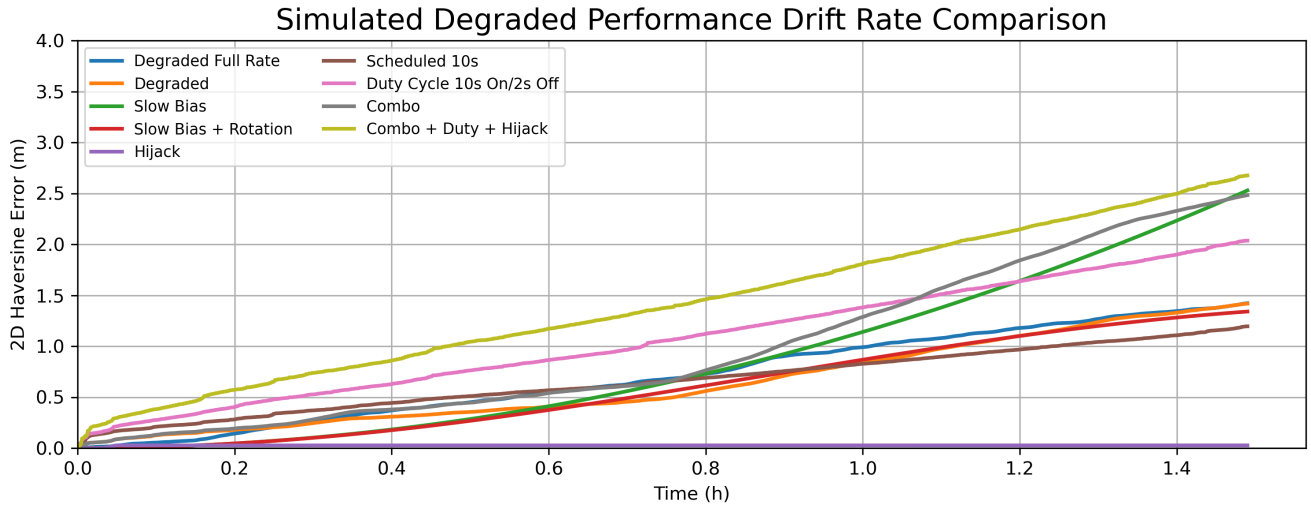

Figure 3. Position error under the "degraded" GNSS model.

Table 3. Summary of GNSS degradation models applied to the example trajectory.

Condition	Description
Degraded	AR(1) correlated noise in position & velocity; inflated covariance.
Degraded + intermittent GNSS	AR(1) correlated noise in position & velocity; inflated covariance. GNSS fixes only every 5 seconds.
Slow bias	Gradual drift in N/E position & velocity; random walk and rotation.
Slow bias with rotation	Gradual drift in N/E position & velocity with rotation.
Hijack	Constant offset applied during a time window (between 30 and 60 minutes).
Reduced rate	GNSS fixes only every 10 seconds.
Duty cycle	GNSS available for 10 seconds, then unavailable for 2 seconds.
Combination degraded and slow bias	AR(1) correlated noise in position & velocity; inflated covariance. Gradual drift in N/E position & velocity; fixes applied every 5 seconds.

Journal of Robotics Research 36(1): 3–15.

Miralles D, Bornot A, Rouquette P, Levigne N, Akos DM, Chen YH, Lo S and Walter T (2020) An assessment of gps spoofing detection via radio power and signal quality monitoring for aviation safety operations. *IEEE Intelligent Transportation Systems Magazine* 12(3): 136–146. DOI:10.1109/MITS.2020.2994117.

Nguyen TM, Yuan S, Cao M, Lyu Y, Nguyen TH and Xie L (2022) Ntu viral: A visual-inertial-ranging-lidar dataset, from an aerial vehicle viewpoint. *The International Journal of Robotics Research* 41(3): 270–280.

Pandey G, McBride JR and Eustice RM (2011) Ford campus vision and lidar data set. *The International Journal of Robotics Research* 30(13): 1543–1552.

Ramezani M, Wang Y, Camurri M, Wisth D, Mattamala M and Fallon M (2020) The newer college dataset: Handheld lidar, inertial and vision with ground truth. In: *2020 IEEE/RSJ International Conference on Intelligent Robots and Systems (IROS)*. IEEE, pp. 4353–4360.

Santamaria E (????) Global navigation satellite system GNSS radio frequency interference .

Schubert D, Goll T, Demmel N, Usenko V, Stückler J and Cremers D (2018) The tum vi benchmark for evaluating visual-inertial odometry. In: *2018 IEEE/RSJ International Conference on Intelligent Robots and Systems (IROS)*. IEEE, pp. 1680–1687.

Shurin A, Saraev A, Yona M, Gutnik Y, Faber S, Etzion A and Klein I (2022) The autonomous platforms inertial dataset. *IEEE Access* DOI:10.1109/ACCESS.2022.3144076.

Smith M, Baldwin I, Churchill W, Paul R and Newman P (2009) The new college vision and laser data set. *The International Journal of Robotics Research* 28(5): 595–599.

Sun K, Mohta K, Pfrommer B, Watterson M, Liu S, Mulgaonkar Y, Taylor CJ and Kumar V (2018) Robust stereo visual inertial odometry for fast autonomous flight. *IEEE Robotics and Automation Letters* 3(2): 965–972.

Wang L, Wu Q, Wu F and He X (2022) Noise content assessment in gnss coordinate time-series with autoregressive and heteroscedastic random errors. *Geophysical Journal International* 231(2): 856–876.

Waymo LLC (2025) End-to-end driving dataset. Technical report.

Yampolsky Z, Stolero Y, Pri-Hadash N, Solodar D, Massas S, Savin I and Klein I (2024) Multiple and gyro-free inertial datasets. *Scientific Data* 11(1): 1080.

Zhang B, Ji D, Liu S, Zhu X and Xu W (????) Autonomous underwater vehicle navigation: A review 273: 113861. DOI:https://doi.org/10.1016/j.oceaneng.2023.113861. URL https://www.sciencedirect.com/science/article/pii/S0029801823002457.

Zuñiga-Noël D, Jaenal A, Gomez-Ojeda R and Gonzalez-Jimenez J (2020) The uma-vi dataset: Visual–inertial odometry in low-textured and dynamic illumination environments. *The International Journal of Robotics Research* 39(9): 1052–1060.